Novel Laser Ablation Resists for Excimer Laser Ablation Lithography. Influence of Photochemical Properties on Ablation

J. Wei,[†] N. Hoogen,[‡] T. Lippert,*[,†] O. Nuyken,[‡] and A. Wokaun[†]

Paul Scherrer Institut, CH-5232 Villigen PSI, Switzerland, and Lehrstuhl für Makromolekulare Stoffe, TU München, Lichtenbergstrasse 4, D-85747 Garching, Germany

Received: September 16, 2000; In Final Form: November 29, 2000

The ablation characteristics of various polymers were studied at low and high fluences. The polymers can be divided into three groups, i.e., polymers containing triazene and ester groups, the same polymers without the triazene group, and polyimide as reference polymer. At high fluences, similar ablation parameters, i.e., etch rates and effective absorption coefficients, were obtained for all polymers. The main difference is the absence of carbon deposits for the designed polymers. At low fluences, very pronounced differences are detected. The polymers containing the photochemically most active group (triazene) exhibit the lowest threshold of ablation and the highest etch rates, followed by the designed polyesters and then polyimide. Neither the linear nor the effective absorption coefficients reveal a clear influence on the ablation characteristics. The thermal properties of the designed polymers also have only minor influence on the ablation activity. The amount of detected gaseous products follows the same trend as the ablation activity, suggesting a combined mechanism of photochemical decomposition and volume increase for the designed polymers. The different behavior of polyimide might be explained by a pronounced thermal part in the ablation mechanism.

Introduction

Laser ablation of polymers was first reported in 1982 and envisioned as a possible alternative or complementary technique to conventional photolithography.[1,2] Laser ablation has the advantage of fewer processing steps, but up to now this potential could not be exploited with the commercially available polymers, such as poly(methyl methacrylate) (PMMA), polyimide (PI), and polycarbonate (PC) etc.[3] These polymers reveal severe drawbacks, such as low sensitivity, carbonization upon irradiation, or ablation debris contaminating the surface and optics. Therefore, novel photopolymers were developed to overcome these limitations.[4−7]

Photochemical considerations have been applied for the design of these polymers. They were designed for an irradiation wavelength of 308 nm, because not all photolithographic processes require a resolution in the submicrometer range, and it is possible to decouple the absorption of the photochemically active groups from the absorption of other parts of the polymer structure. This concept can be used to test whether the incorporation of photochemically active groups into the polymer chain improves the ablation characteristics. The XeCl excimer laser (308 nm) is a technically interesting tool, due to the long lifetime of gas fills and laser optics. The most promising approach for the design of these "laser ablation polymers" is the incorporation of the photochemically active chromophore into the polymer main chain. In this way, the polymer is highly absorbing at the irradiation wavelength and decomposes exothermically at well-defined positions of the polymer chain into gaseous products.[8,9] The gaseous products act as driving gas of ablation and carry away larger fragments, which could otherwise contaminate the surface. The polymers are therefore ablated without major modifications of the residual polymer surface, thus allowing a reproducible ablation.[10]

From the standpoint of ablation properties, triazene groups (−N═N−N⟨) containing laser resists have been identified as the most promising candidates. Unfortunately, problems are encountered with the stability with respect to the following steps during a complete processing cycle, e.g., oxidation of the substrate.[11] Selected polyesters (PE) and polyester carbonates (PEC) have also been found to exhibit good ablation behavior.[12] The sensitivities of the PE's and PEC's are lower as compared to the triazene-based polymers, but they exhibit a higher chemical stability. These polymers also produce small gaseous products (CO_2, CO) upon decomposition.

Introducing a functional ester group that enables selective photo-cross-linking without destruction of the polymer backbone can improve the stability of the polymers without changing the sensitivity to direct laser structuring.[13] These polymers can function as positive (laser ablation) as well as conventional negative resists. An application could be envisioned where first a "large" scale structuring, using standard negative resist methods, is followed by a positive (i.e., laser ablation) step to structure the remaining areas in more detail. The order of processing can be reversed without altering the quality of the structures.[14] Combined positive−negative resists are a new concept which to our knowledge has only been reported once for the positive-negative inversion of poly(di-*n*-hexylsilane) upon ion beam irradiation.[15] First results about laser ablation of the combined positive negative resists were reported recently.[14]

Novel polymers were synthesized to test whether it is possible to combine the sensitivity of the triazene polymers with the stability of the polyesters. These polyesters contain cinnamylidenemalonyl groups as cross-linking units and the triazene functional group. To compare the influence of these two chromophores (triazene vs ester), polymers were synthesized

* Corresponding author. Fax: 0041-56-310-2485. E-mail: thomas.lippert@psi.ch.
[†] Paul Scherrer Institut.
[‡] TU München.

10.1021/jp003325a CCC: $20.00
Published on Web 01/20/2001

SCHEME 1: Chemical Structures of the Polymers

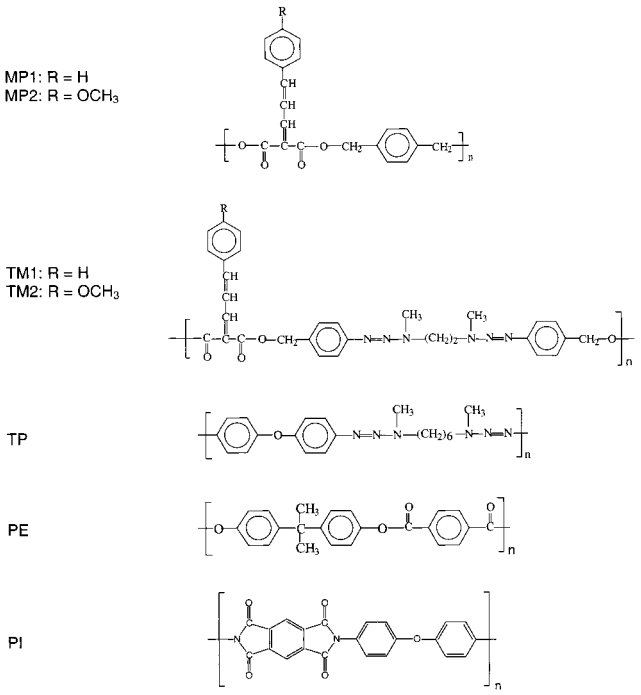

containing the same ester group but with and without the triazene groups. Cinnamylidenemalonic acid is known to photodimerize via (2+2)-cycloaddition with $\lambda_{irr} > 395$ nm.[16] At these irradiation wavelengths neither the triazene groups nor the ester groups are decomposing. The chemical structures of the new polymers TM1, TM2, MP1, and MP2 are shown in Scheme 1. TM1 and TM2 contain triazene functional groups, whereas MP1 and MP2 are the polyesters without the triazene groups. To compare the ablation properties of the new polymers, several other polymers were included as references in this study, i.e., polyimide (PI, Kapton from Goodfellow) as representative of a highly absorbing "standard" polymer, a commercial polyester (PE, APE 100 Bayer AG) as representative of standard ester polymers, and TP, as representative of the original triazene polymer, without the photo-cross-linkable ester group.

Experimental Section

The polymers, TM1, TM2, MP1, and MP2, were synthesized using a standard polycondensation reaction. The synthesis is described in detail elsewhere.[17] Photo-cross-linking of the polymers was realized by the irradiation at $\lambda > 395$ nm for 20−40 min at a irradiance of 100 mW cm^{-2}, resulting in cross-linking yields of greater than 50%. After cross-linking, the polymers are named TM2C, MP1C, and MP2C.

A series of thin polymer films were cast on quartz substrates with various thicknesses (around 100 nm) to determine the linear absorption coefficients of the polymers. The absorption of the films was measured at 308 nm using a UV spectrometer (Polytec XDAP), while the exact thickness of the films was determined by a surface profiler (Dektak 8000). The linear absorption coefficients, α_{lin}, obtained by this method are compiled in Table 1, together with the molar absorption coefficients, ϵ, measured in THF.

A XeCl excimer laser (Lambda Physik, Compex 205; $\lambda =$ 308 nm, $\tau = 20$ ns) was used as irradiation source. The polymer films (50 μm thick) for the laser ablation experiments were prepared by solvent casting with THF as solvent. To determine the etch rates of the polymers, a pinhole mask (diameter = 4 mm) was demagnified with a lens ($f = 100$ mm) onto the polymer surface to create circular craters. The pulse energy deposited on the sample was measured by a joulemeter (Gentec 200). The fluence for a constant spot size was varied between 10 mJ cm^{-2} and 10 J cm^{-2} using a dielectric attenuator (Laser Laboratorium Göttingen) and an additional beam splitter (10% transmission) for the low fluences. The number of pulses delivered to the sample was controlled by a pneumatic shutter. For a typical experiment, a 10 × 10 matrix of circular craters was created on every polymer film, while varying the fluence and the pulse number. All ablation experiments were performed in air. The depth of the ablated craters was measured with the surface profiler. The ablation experiments were performed at low (10−400 mJ cm^{-2}) and high fluences (0.5−10 J cm^{-2}) to investigate the ablation behavior of the polymers over a broad fluence range.

To analyze the gaseous ablation products and fragments, a vacuum chamber equipped with a quadrupole mass spectrometer was used. The laser beam was focused onto the sample surface through a quartz window using a lens with a focal length of 40 cm. The sample was tilted 45° with respect to the incoming laser beam, while the detector of the mass spectrometer is perpendicular to the laser beam at a distance of approximately 1.5 cm.

For the microstructuring experiments, a copper mask (diameter = 3 mm) with a slit pattern was used. The mask consists of two different slits with widths of 100 and 60 μm. The mask was imaged by a Schwarzschild type reflecting objective (Ealing; demagnification, 15×) onto the polymer surface to avoid lens aberration. The quality of the ablated structures was evaluated by scanning electron microscopy (SEM).

Results

Physical Properties of the Polymers. All polymers in this study can be classified as highly absorbing polymers ($\alpha_{lin} \geq$ 8000 cm^{-1} at the irradiation wavelength of 308 nm), as shown in Table 1. Cross-linking reduced the absorption coefficient only slightly for the triazene-containing polymer, while for MP1 a very pronounced reduction was observed. The novel polymers were especially selected according to the criterion of similar α_{lin}, which would allow a direct comparison of the polymers. This could be accomplished for the high end of absorptivity for four different polymers, i.e., TP, TM2, MP1, and PI. The glass transition temperature, T_g, are very similar for all designed polymers, i.e., 63 °C for TP, 73 °C for TM1, 79 °C for TM2, 64 °C for MP1, and 74 °C for MP2. The cross-linked polymers reveal no T_g. The decomposition temperatures range from 227 °C for TP, 245 °C for TM1, 248 °C for TM2 to 321 °C for MP1, and 327 °C for MP2 to around 500 °C for PI. This shows that the decomposition temperature of the bifunctional polymers (triazene + ester group) are governed by the triazene group.

Ablation at High Fluences (0.5−10 J cm^{-2}). The etch rates (etch depth/pulse) at high fluences were calculated from linear plots of the etch depths vs pulse number at a given fluence. All plots were linear, showing no incubation behavior as expected for highly absorbing polymers. The etch rates versus the natural logarithm of the fluence are shown for all polymers in Figure 1a. The etch rates increase approximately linearly at lower fluences (0.5−6 J cm^{-2}). The highest etch rate of. 2.3 μm/pulse at a fluence of 10 J/cm^2 was measured for TCP1, but the difference to the etch rates of the other polymers is quite small. The triazene-containing polymers exhibit slightly higher etch rates than the non-triazene-containing polymers. Photo-cross-linking has only minor effects on the etch rates at high fluences

TABLE 1: Chemical Properties and Ablation Parameters of the Polymers

	α_{lin}[a] (cm^{-1})	ϵ_{308}[c] (M^{-1} cm^{-1})	$\alpha_{eff}(LF)$[d] (cm^{-1})	$F_{th}(LF)$[e] (mJ cm^{-2})	$\alpha_{eff}(HF)$[f] (cm^{-1})	$F_{th}(HF)$[g] (mJ cm^{-2})
MP1	102 000	27 400	50 700 ± 2100	63 ± 3	16 200 ± 700	343 ± 42
MP1C	39 000[b]	n.m.	49 000 ± 2700	66 ± 4	17 200 ± 800	323 ± 43
MP2	32 000	7100	57 000 ± 2000	48 ± 3	20 600 ± 1800	269 ± 59
MP2C	17 000[b]	n.m.	57 600 ± 3200	53 ± 3	22 800 ± 1600	229 ± 40
TM1	69 000	57 000	56 100 ± 3400	27 ± 2	14 400 ± 900	410 ± 46
TP	100 000	27 700	49 800 ± 2900	27 ± 2	16 700 ± 1100	317 ± 63
TM2	92 000	35 600	53 300 ± 2500	28 ± 2	18 500 ± 1200	225 ± 40
TM2C	81 000[b]	n.m.	49 700 ± 2300	31 ± 3	18 600 ± 1300	236 ± 36
PI	95 000	n.m.	83 300 ± 3400	60 ± 3	17 400 ± 1500	508 ± 65
PE	8000	1000	51 500 ± 3200	73 ± 4	19 200 ± 1600	340 ± 60

[a] Linear absorption coefficient at 308 nm determined by UV spectroscopy and profilometry. [b] Linear absorption coefficient at 308 nm calculated from UV-spectroscopical data after photo-cross-linking. [c] Molar absorption coefficient measured in solution. n.m.: not measured. [d] Effective absorption coefficient calculated from eq 1 at low fluences. [e] Threshold fluence calculated from eq 1 at low fluences. [f] Effective absorption coefficient calculated from eq 1 at high fluences. [g] Threshold fluence calculated from eq 1 at high fluences.

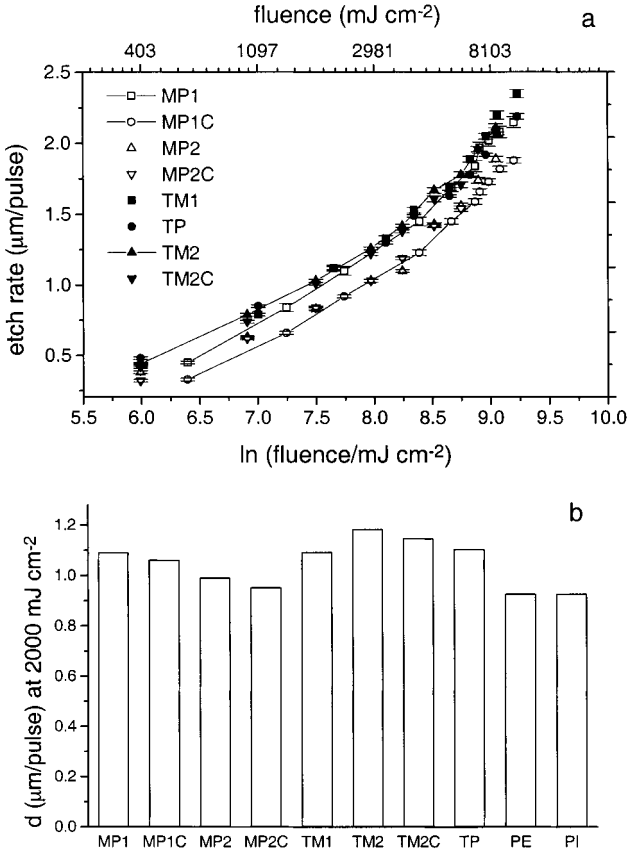

Figure 1. (a) Measured etch rates as a function of natural logarithm fluence at high fluences (0.5−10 J cm^{-2}). (b) Calculated etch rates of all polymers at 2000 mJ cm^{-2}.

as shown by the very similar etch rates determined before and after photo-cross-linking.

The ablation parameters, α_{eff} (effective absorption coefficient) and F_{th} (threshold fluence) were calculated according to the eq 1[18,19]

$$d(F) = \frac{1}{\alpha_{eff}} \ln\left(\frac{F}{F_{th}}\right) \quad (1)$$

where $d(F)$ is the etch rate (etch depth per pulse). The calculated values for α_{eff} and F_{th} are summarized in Table 1 and are quite different from the values obtained at low fluences (see below and Table 1). The effective absorption coefficient, which is a measure for the penetration depth of the laser, depends strongly on the applied laser fluence. Several factors can account for this fact; i.e., the incoming photons are absorbed by ablation products in the gas phase and polymer film. These products can be either neutrals or, more likely, radicals. At higher fluences and therefore greater ablation depths, more products are formed. The absorption is also dependent on the lifetime of the products.[20] The lifetime is strongly dependent on the complexity of the molecules. The more complex the molecule the longer the lifetime. In the condensed phase as in the case of PI, such radical intermediates can persist for time periods of the order of nanoseconds (laser pulse ≈ 20 ns). The importance of this fact to the UV-laser decomposition of, e.g., PI, lies in the UV-absorption characteristics of free-radical intermediates. Their strongly delocalized electrons will result in a more intense absorption of the incoming radiation than PI itself. Their contribution to the absorption will be determined by their stationary concentration, i.e., the ratio of their rate of formation to their rate of disappearance. The other important factor is the absorption of the incoming photons by the laser-created plasma, which is observed at high fluences. The absorption of the incident laser radiation is quantitatively described in the model of the moving interface by Lazare et al.[21,22] In general, lower effective absorption coefficients compared to the linear absorption coefficients are obtained, which suggests that bleaching[23,24] and/or decomposition of the absorbing chromophore takes place during irradiation.[25]

The calculated etch rates[26] (eq 1) at 2000 mJ/cm^2 of polymers are shown in Figure 1b. The etch rates of the triazene-containing polymers, TM1, TM2, and TP, are around 1100 nm/pulse, which is slightly higher than for the non-triazene-containing polymers, MP1 and MP2. The polyester PE and polyimide (PI) exhibited slightly lower etch rates (≈900 nm).

The morphology of the polymer films after laser ablation was examined using a scanning electron microscope (SEM). In Figure 2 the SEM micrographs of the structures in TM2 and MP2C are shown as examples. Generally, well-defined circular craters are created on all polymers with the exception of MP2C. Sharp edges and smooth bottoms are obtained, as shown in Figure 2a, indicating no pronounced thermal damage. Almost no ejected material is deposited around the craters. A clean surface is important for the application of laser ablation in lithography. In the case of MP2C, craters with lower structural quality are obtained for fluences above 7 J cm^{-2}. The resulting craters are very irregular as shown in Figure 2b. The diameter is about 600 μm, which is much larger than the 280 μm diameter of the beam and of the craters in the other polymers. A similar phenomenon was observed for TP in a previous study.[5] It has been suggested that the larger crater is due to a shock wave,

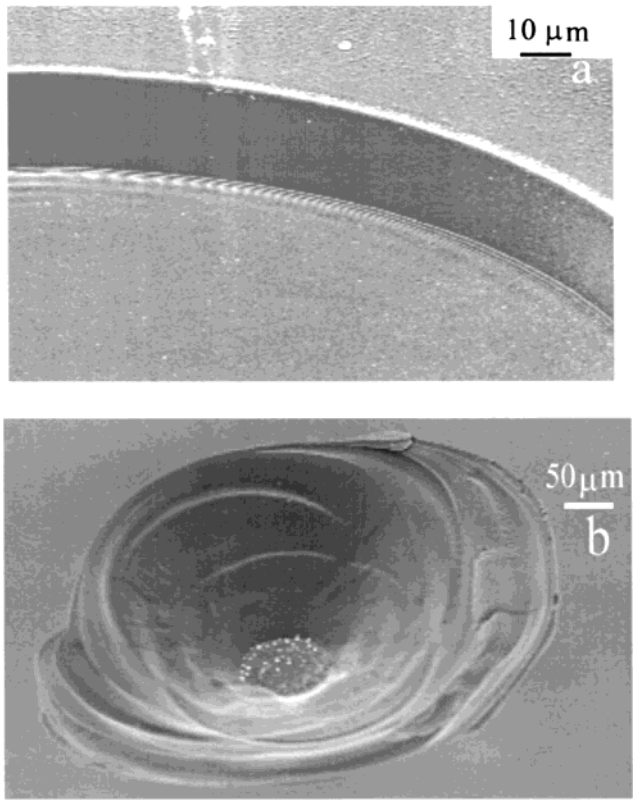

Figure 2. SEM micrographs of craters ablated with high fluences: (a) TM2 irradiated at 8.5 J cm^{-2} with 10 pulses; (b) MP2C irradiated at 7.3 J cm^{-2} with 11 pulses.

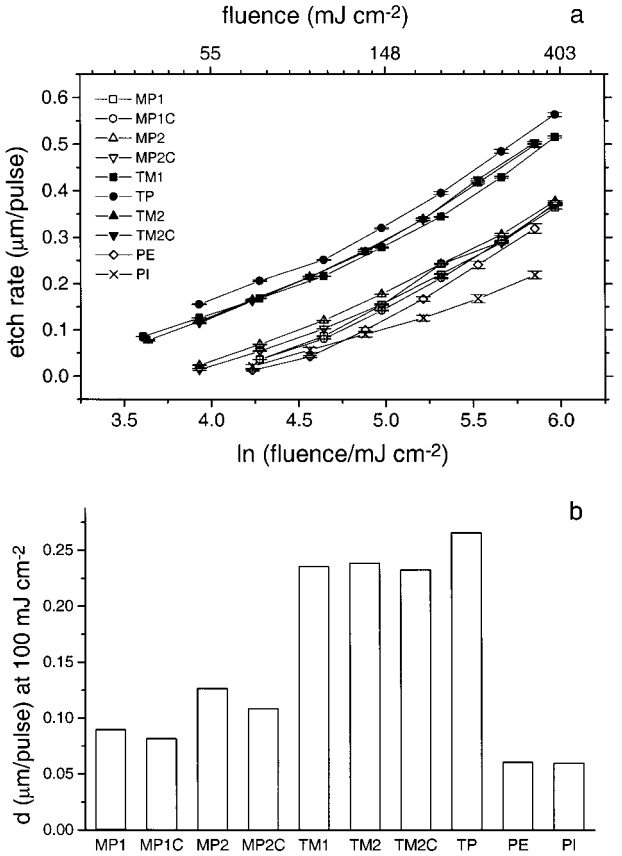

Figure 3. (a) Etch rates at low fluences (up to 400 mJ cm^{-2}) as a function of the natural logarithm of the laser fluence. (b) Calculated etch rates at 100 mJ cm^{-2} for all polymers.

which was created by the ablation process. The shock wave is reflected from the substrate, causing the spallation of a larger area of the polymer film. Shock waves in the polymer film of TP were also detected previously.[25] However, no such irregular craters are observed for TM1, probably due to a different thickness of the polymer film. Regular craters are obtained in MP2C for fluences lower than 7 J cm^{-2}, indicating a threshold fluence for the creation of these large damages.

Ablation at Low Fluences (up to 400 mJ cm^{-2}). The high fluence range is mainly interesting for applications where high ablation rates in small areas are important, e.g., drilling or cutting. The low fluence range offers the opportunity to study the influence of structural parameters on the ablation rates. The low fluence range is also important for lithographic applications, where the cost of the photons is important. Low fluences are defined in this study from 10 to 400 mJ cm^{-2}. The etch rates were determined according to the procedure described for the high fluence. Linear plots of the etch depths vs the pulse number were also obtained. A plot of the etch rates versus the natural logarithm of the fluences is shown in Figure 3a. A satisfactory linearity between etch rates and the logarithm of fluence is obtained. The designed polymers (MP's, TM's, and TP) can be divided into two groups with respect to the etch rates (shown in Figure 3a). All triazene-containing polymers have significantly higher etch rates than the other polymers. The designed polyesters (MP's), as well as PE, reveal a higher etch rate than PI. The etch rate is independent of α_{lin} (see Table 1) and determined by the chemical structure. In Figure 3b a comparison of the calculated etch rates at 100 mJ cm^{-2} is shown for all polymers. The etch rates of non-triazene-containing polymers, MP1 and MP2, are approximately 100 nm/pulse, which is about half the value of the triazene-containing polymers, TM1, TM2, and TP. A slightly higher etch rate is obtained for TP, which has the highest triazene density per polymer chain. The etch rates of the polyester (PE) and polyimide are about 60 nm/pulse which is again about half of the value of the designed polyesters. This is remarkable because the linear absorption coefficients of the designed polyesters (including the cross-linked) cover the same broad range as PE and PI.

The effective absorption coefficient α_{eff} and threshold fluence F_{th} were calculated according to eq 1 and are summarized in Table 1. The effective absorption coefficients, α_{eff}, calculated at low fluences, are much larger than the values obtained at high fluences. The effective absorption coefficients do not correlate with the linear absorption coefficients (Table 1), maybe with the exception of PI. A difference between the values of α_{eff} and α_{lin} is observed for most polymers. An important feature is the similarity of α_{eff} for all designed polymers, including PE ($\approx$54 000 $\pm$ 5000 cm^{-1}), while PI reveals a much higher value (Table 1).

From an economic point of view, a polymer with a threshold fluence as low as possible is most desirable. The threshold fluences of the triazene-containing polymers, TM1, TM2, and TP, are about 30 mJ/cm^2, which is much lower than those for the non-triazene-containing polymers, MP1 and MP2 ($\approx$60 mJ cm^{-2}). These values are, to our knowledge, the lowest threshold fluence reported for laser ablation of polymers at 308 nm. The threshold fluence of TP obtained from this study is in good agreement with the value determined previously by UV-spectroscopy.[23] The calculated threshold fluences (from eq 1, shown in Table 1) agree also very well with the experimentally observed threshold[27] fluences. The threshold fluences of the cross-linked polymers are slightly higher than for non-crosslinked polymers (see Table 1), suggesting that cross-linking has a minor influence on the ablation properties of the polymers.

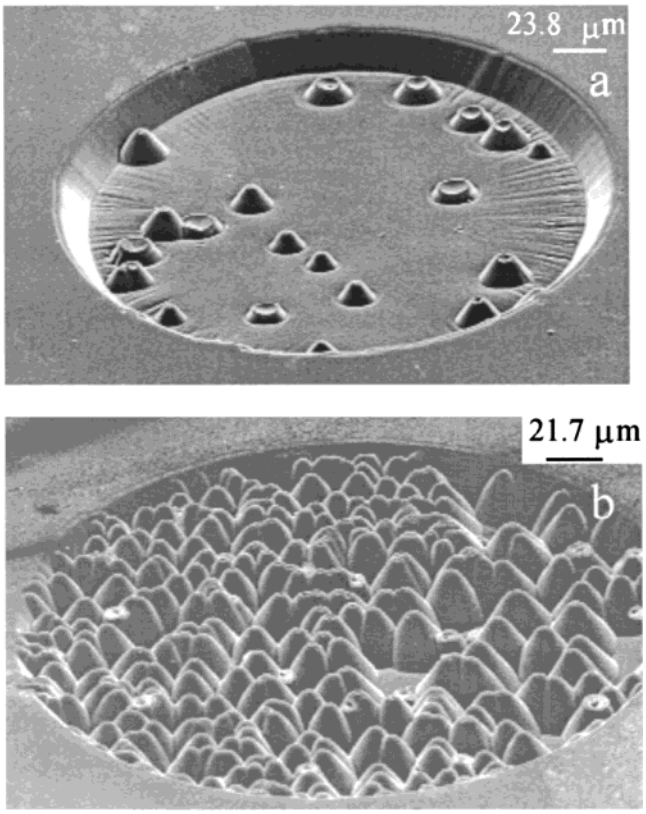

Figure 4. SEM micrographs of ablated craters at low fluences: (a) crater in TM2, irradiated at 69 mJ cm^{-2} with 88 pulses; (b) crater in MP2C irradiated at 51 mJ cm^{-2} with 200 pulses.

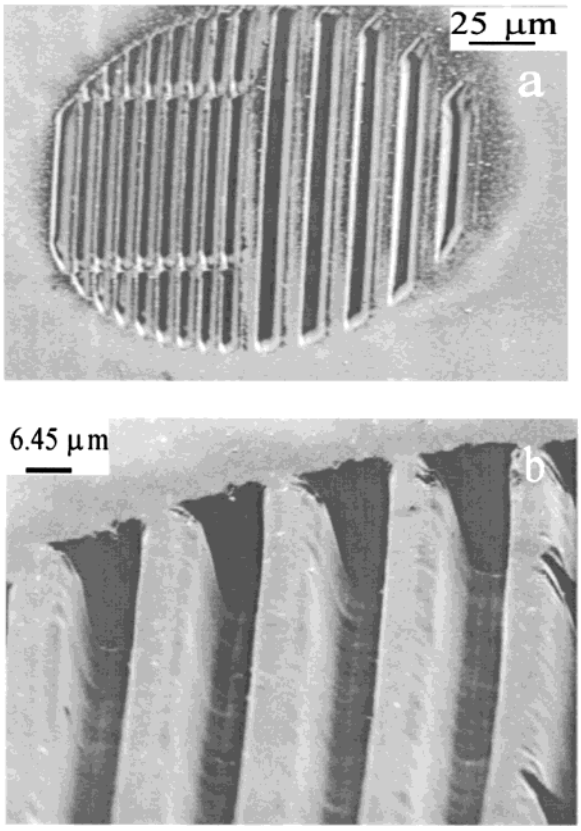

Figure 5. SEM micrographs of microstructures: (a) structure in MP2C irradiated at 4.6 J cm^{-2} with 9 pulses; (b) structure in TM2C irradiated at 4.6 J cm^{-2} with 11 pulses.

The appearance of the craters obtained at low fluences varies partly from the morphologies of the craters formed at high fluences. Figure 4 shows the craters created on TM2 at fluences of 69 and 51 mJ cm^{-2}, respectively. Conical structures were observed in both cases at the bottom of the circular craters. The number of cones decreases dramatically by increasing the fluence, indicating a fluence range for obtaining these cone structures. The number of cones increases also with the number of laser pulses at a fluence within the above-described range. No cones are observed after laser irradiation, in the case of TM2, if the fluences are higher than 80 mJ cm^{-2}. The formation of conelike structures within a certain fluence range was observed previously for other polymers, e.g., PI.[28] The formation of the cones has been assigned to impurities in the polymer.[29,30] These impurities have a higher ablation threshold than the polymer, which results in shading of the underlying polymer by the impurity particles, causing the formation of the cone structures. If the fluence is increased above a certain value, which corresponds to the threshold fluence of the impurity material, smooth ablation surfaces are obtained again. In the case of PI, calcium was detected as impurity by energy-dispersive X-ray analysis (EDX). Graphitic carbon was found by Raman microscopy on top of the calcium, at the tip of the cones.[31] For TM2C, carbon was neither detected on top of the cones nor in the surrounding of the ablated craters, using Raman microscopy. This indicates that carbonization during laser ablation of the polymer is not the reason for the creation of the cones and that "clean" ablation can be achieved with the triazene-containing polymers. This was also confirmed previously for TP by analyzing the surface after ablation with X-ray photoelectron spectroscopy (XPS).[10] The "clean" ablation is an important feature for practical applications, because carbonization of the polymer surface will alter the ablation characteristic and therefore reduce the reproducibility of ablation. The elemental composition on top of cones was determined with EDX for TM2, and Si, O, and Cl were identified as impurities. The formation of the cones in TM2 is therefore most probably also due to impurities in the polymer. Cone structures were also observed after ablation of the other polymers, but at slightly different fluences and in smaller numbers. This can be explained by different quantities of impurities within different polymers.

Microstructuring of Polymers. A microstructure with broad (ca. 8 μm) and narrow (ca. 4 μm) channels was created in the polymers to demonstrate the possibility of structuring the polymers with a resolution in the micron range. High-quality microstructures can be created on all designed polymers as shown for MP2C and TM2C in Figure 5. The SEM micrograph with the higher magnification (Figure 5b) reveals nearly no debris in the areas surrounding the structure. The structures have flat bottoms and the remaining ridges are well-defined. The depths of channels can be controlled by fluence and/or pulse number. The experimental results show that the designed polymers are suitable for microstructuring and exhibit structures with similar qualities. With an improvement of the experimental setup, it should be possible to create various microstructures with an even higher resolution.

Measurement of Gaseous Products during Laser Ablation. It is very important, as discussed above, that the ablation products or debris are not contaminating the polymer surface and optics. It has been suggested that a large amount of gaseous products is necessary to achieve this goal. The neutral gaseous products and fragments of laser ablation were analyzed with quadrupole mass spectroscopy as described in the Experimental Section. The ablation experiments were performed with TM1 and MP1 in the low and high fluence ranges, i.e., at 130 and 540 mJ cm^{-2}. The detected masses (after electron impact

TABLE 2: Gaseous Products Determined with a Modified Quadrupole Mass Spectrometer[a]

m/*z*	fragment	rel intensity of peaks in % MP1	rel intensity of peaks in % TM1
12	C	11	6
14	N	5	10
	CH_2		
15	CH_3	15	35
16	CH_4	24	19
	O		
25	C_2H	29	9
26	C_2H_2	100	43
27	C_2H_3	20	51
28	C_2H_4	56	100
	CO		
	N_2		
39	C_3H_3	26	6
44	CO_2	100	10
50	C_4H_2	30	2
51	C_4H_3	18	1

[a] The ablation experiment was performed at a fluence of 130 mJ cm^{-2}.

ionization with 70 eV), their relative intensities, and suggested elemental compositions are shown for a fluence of 130 mJ cm^{-2} in Table 2. The detected masses are of course a mixture of primary or direct ablation products, and secondary products resulting from reactions in the ablation plume as well as from fragmentation induced by the electron impact ionization. The C_xH_y structures, e.g., C_2H_x, C_3H_x, and C_4H_x, are typical products of the fragmentation of aromatic compounds. With the given data it is impossible to determine whether these are primary or secondary products. In the case of the triazene-containing polymer, TM1, the main product has a mass of $m/z = 28$, corresponding either to N_2, CO, or C_2H_4. All these species might be produced during laser ablation. Our experimental setup does not have the resolution to distinguish between these isotopic variants. However, a time-of-flight mass spectrometry study of TP shows that the main ablation product is N_2.[9] This suggests that, in the case of TM1, N_2 may also be the main product. Nitrogen as main product is consistent with a laser-induced decomposition mechanism of the triazene molecules. The primary decomposition step is the homolytic bond breaking between the nitrogen atoms N^2 and N^3 of the triazene group, forming a very reactive azoradical from which N_2 is eliminated. For MP1, the main products, with identical intensity, are CO_2 and C_2H_2. This is consistent with quantum chemical calculations showing that absorption at the irradiation wavelength occurs within the whole cinnamylidenemalonyl group, causing the decomposition of this structure into the above-described fragments. The same fragments are also detected for TM1, but with lower intensities. It is noteworthy to mention that the overall intensity of all fragments is 10 times higher for the triazene-containing polymers. This is consistent with the higher ablation rates of the triazene polymers and the suggested role of gaseous products as driving/carrier gas of ablation.

Photochemical Properties. A simple experiment was performed to compare the photochemical activity of the MP with the TM polymers. Solutions of TM1 and MP1 in quartz cuvettes with the same absorptivity were irradiated with 60 mJ cm^{-2}. The UV−vis spectra before and after irradiation are shown in Figure 6. A comparison of the absorption bands after 100 pulses shows that about 50% of TM1 and only 20% of MP1 are decomposed. This confirms clearly that the triazene-containing polymers decompose photochemically much easier than the polymers without this group. It is important to point out that

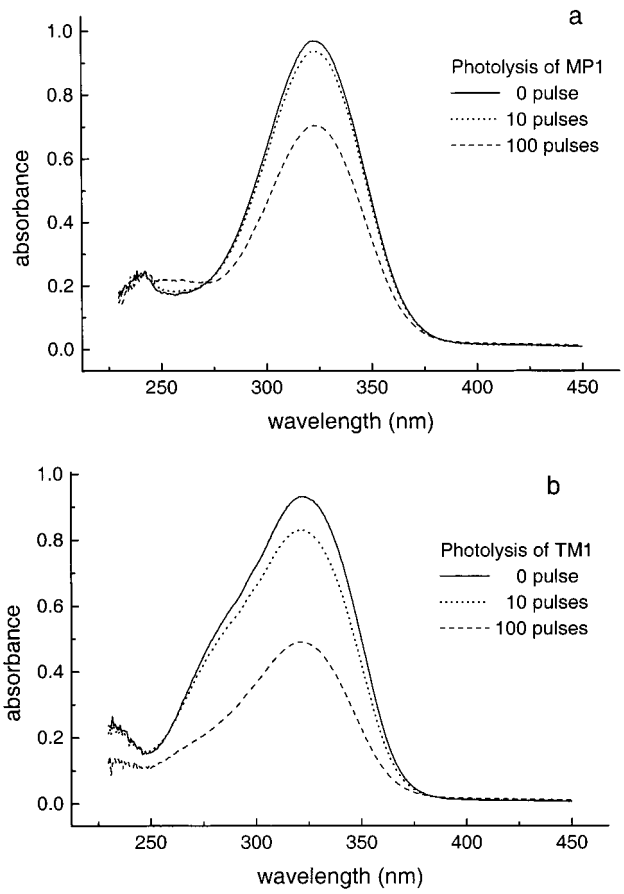

Figure 6. UV spectra recorded after irradiation of MP1 and TM1 in THF. 1.2 mL of solution (ca. 10^{-5} M) was irradiated by laser pulses with energy of 110 mJ.

TM1 contains the same structural unit as MP1 (Scheme 1), but with the additional triazene unit in the repetition unit of the polymer. Irradiation of low concentrations of the polymer in solution can be interpreted as pure photochemical decomposition with nearly no thermal influences.

Discussion

The experiments at high fluences reveal that under these conditions the material properties of the polymers are only of minor importance. All polymers have very similar ablation rates, which indicates that with the excess of laser energy and photons, similar processes govern the ablation behavior. It is most probable that the polymers decompose into similar small products and that the created plasma is also comparable. This was also suggested by emission spectroscopy, confirming that the main species in the plasma are CN, C_2, and CH species for all polymers. The plasma and the products of ablation shield the incoming laser radiation, which limits the etch rates. This is observed for the triazene polymers at fluences >12 J cm^{-2} (not shown in Figure 1). At these high fluences the etch rates are more or less constant. Therefore, similar ablation parameters are derived for all polymers including the two reference polymers PI and PE. The only important difference between the ablation characteristics is the deposition of debris in the surrounding of the ablation contours. In case of PI, carbon deposits are detected in the surrounding of the polymers. The thickness of the deposits increases with pulse number, while the area of deposition increases with fluence and only slightly with pulse number.[31] Inside the ablation feature carbonization is also detected. As mentioned above, this carbonization will

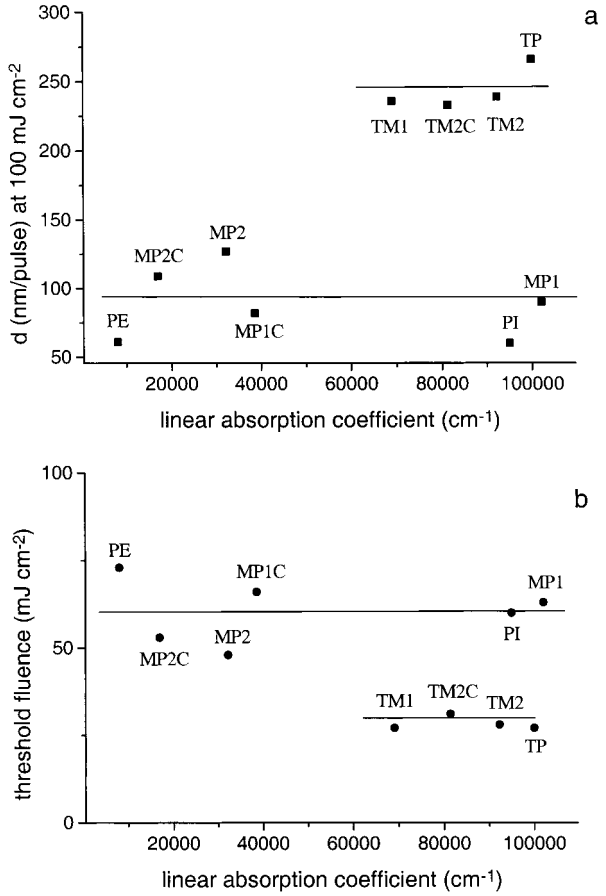

Figure 7. Influence of the linear absorption coefficients at the laser wavelength on (a) the etch rates at 100 mJ cm^{-2} and on (b) the threshold fluences. The lines in the figure are just for guiding the eyes.

alter ablation characteristics, thus making the whole ablation process less predictable. The deposition of the carbon debris is of course also of concern for optical components, which are in the vicinity of the ablation sites. Contrary to PI, no deposits in the surrounding or inside the ablation crater are detected for the triazene-containing polymers. This reveals the superior properties of the designed polymers. Two explanations might be offered for this behavior. The content of aromatic systems is lower in the triazenepolymers as compared to PI. The small decomposition fragments of aromatic systems, such as C_2, are thought to be the "building stones" of carbonization. Another, maybe more important, feature is the high amount of gaseous fragments obtained by laser ablation of the designed polymers. These gaseous fragments act as driving gas of ablation and carry away the carbon fragments. It has been shown with TOF-MS for TP that N_2 is the major product (factor of 15 higher intensity than for other products) of ablation. This inert product is entraining other products, proving the carrier gas concept. The carbon fragments are carried away in the nitrogen, which might even act as diluent, rendering the recombination of the carbon fragments more difficult.

At low fluences a pronounced difference between the polymers can be detected. The tested polymers can be roughly divided into three groups: the polymers containing the triazene group, the polyesters (may be with inclusion of PE into this group), and PI. The triazene-containing polymers have by far the highest activity (highest etch rate and lowest threshold fluence) to laser ablation, followed by the polyesters and then PI. A comparison of all polymers is shown in Figure 7. The linear absorption coefficients of the polymers are plotted against the etch rate at a fluence of 100 mJ cm^{-2} (Figure 7a) and against the threshold fluence (Figure 7b). Among the triazene-containing polymers TP reveals the highest activity, probably due to the highest density of triazene groups in the polymer chain, resulting in larger amounts of nitrogen as product. The same order of activity is also confirmed by other experimental techniques, i.e., irradiation of the polymer in solution (Figure 6) and mass spectrometry. The triazene-containing polymers decompose much faster during irradiation in solution, where thermal effects should be of only minor importance. In the mass spectroscopy studies a much higher amount of gaseous products is detected for the triazene-containing polymers, confirming of course the higher etch rates, but also the role and importance of the gaseous species. These very pronounced differences are even more remarkably if we consider that the polymers were selected for similar absorption properties. At least one polymer out of each group has a comparable, linear absorption coefficient (97 000 $\pm$ 5000 cm^{-1}), i.e., TP and TM1 for the triazene-containing polymers, MP1 for the designed polyesters and PI for the reference polymers (see Figure 7). This ensures that a direct comparison of these polymers is possible, due to the deposition of the laser energy within the same volume of the polymer. If the effective absorption coefficient is considered, then the triazene polymers can still be compared to the polyesters because their values are again quite similar (54 000 $\pm$ 5000 cm^{-1}). Only PI reveals a quite different effective absorption coefficient, similar to the value of the linear absorption coefficient. Whereas the effective absorption coefficients are comparable, very pronounced differences between the triazene-containing polymers and the polyesters are obtained for the ablation activity. This suggests that α_{eff} is of only minor importance for the ablation performance. The same is true for the linear absorption coefficients, because a variation of α_{lin} within one group of polymers has again no pronounced influence as seen when comparing, e.g., MP1 and MP2 (see Figure 7). It is probably more important for its value to lie above a certain threshold (approximately 10 000 cm^{-1}), where direct ablation without incubation is observed. Of course one might argue that the same order of activity is also obtained if only the decomposition temperatures (T_{dec}) are considered, i.e., lowest T_{dec} for the triazene polymers, followed by the polyesters and then PI. However, a comparison reveals that the largest difference in thermal stability (170 °C) between polymers of different groups, i.e., PI and MP1, corresponds to the smallest difference in ablation activity, while the smallest difference in thermal stability (70 °C), between TM2 and MP1, corresponds to the largest difference in ablation activity. This is even more remarkable when recalling that this inequality is valid in a broad fluence range (from 10 to at least 400 mJ cm^{-2}), which covers a quite broad thermal range. This suggests that thermal considerations are less important for the laser ablation of these polymers. Just using the decomposition temperatures is of course a simplification, because other parameters such as thermal conductivity, specific heat, thermal diffusivity, etc. are also important. Looking at the chemical structure of the polymers shows that all polymers have at least common parts in their chemical structure, suggesting that they might have comparable values for these constants, and hence justifying the simplification. Together with the experiments in solution, where concentration in the 10^{-5} molar range of the polymers are used, this suggests an only minor part of a thermal mechanism.

Now we would like to take a step back and look in more detail at some fundamental, photochemical aspects of laser ablation. The photon energy of the XeCl excimer laser is 4.02

SCHEME 2: Possible Decomposition Mechanism of the Polymers TM1 and MP1[a]

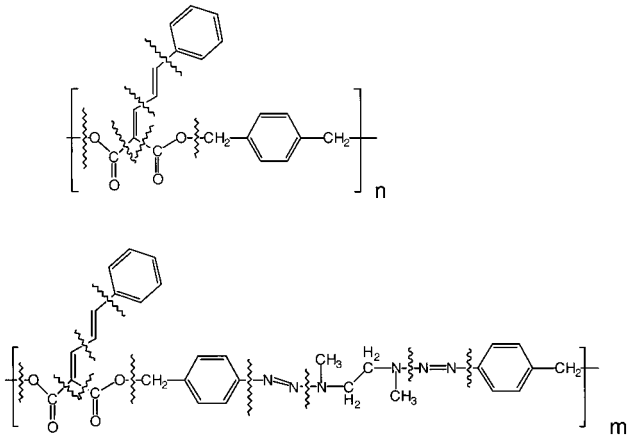

[a] Resulting fragments are identified in the mass spectra.

eV, which is just above the binding energy of C−C (3.6 eV), C−N (3.2 eV), and C−O (3.7 eV) bonds, but clearly above the value of the N−N bond (1.7 eV).[32] This suggests that direct photochemical breaking of these bonds is at least possible. Quantum chemical calculations have shown that the triazene chromophore is responsible for the absorption at 308 nm,[23] and photochemical studies of monomeric triazene identified the N−N bond as initial photodecomposition site.[33] The fragments found in the MS analysis of the triazene polymers are also compatible with this mechanism (Scheme 2). The differences between PI and the polyesters can be explained in two ways. Quantum chemical calculations have shown that the absorption at 308 nm in the designed polyesters is due to the entire cinnamylidenemalonyl group, which is, according to the fragments, also the preferential decomposition site, yielding e.g. CO_2 and C_2H_2 as main fragments. (A possible decomposition scheme is shown in Scheme 2.) The absorption at 308 nm is less localized for polyimide, and the imide system as well as the oxygen of the biphenyl ether groups have been identified as primary decomposition sites.[34] This, together with lower amount of gaseous products, might be responsible for the lower ablation activity. The amount of gaseous products follows the same order as the ablation activity, i.e., triazene polymers > polyesters > PI. The second, more probable reason for the low ablation activity of PI is that decomposition of PI proceeds according to purely photothermal mechanism,[35] as suggested by a theoretical model.[36] For the designed polymers a mechanism might be active, which combines the photochemical activity with the resulting pressure/volume increase of the gaseous fragments inside the polymers.

One interesting point worth analyzing in more detail is the quite similar effective absorption coefficients for all designed polymers, which are independent of the linear absorption coefficients. The effective absorption coefficient of PI is different from the more or less constant values of the designed polymers and is similar to the linear absorption coefficient. This might also be an indication for different ablation mechanisms acting for PI and the designed polymers. All designed polymers are supposed to decompose according to a similar mechanism, i.e., direct photolysis, during which homolytic bond breaking occurs. Radicals are formed as intermediates, such as phenyl radicals, which might be present for all designed polymers. These radical intermediates would limit the effective absorption coefficient for all polymers to a similar value. In the case of PI different intermediates might be formed, e.g., ionic species, which should have quite different absorptivities, resulting in the different effective absorption coefficients. Another possibility of explanation invokes the thermal route of decomposition of PI, which would take place immediately after the laser pulse. In this case, the modifications of the ablated polymer surface, e.g., the carbonization, or the higher temperature of the remaining polymer might be responsible for the difference between the linear and effective absorption coefficient.

A detailed analysis of the ablation characteristics of cross-linked vs not cross-linked polymers reveals that for the cross-linked polymers consistently lower ablation activities are obtained. This is probably due to the higher mechanical stability and larger viscosity of the cross-linked polymers. The latter observation is consistent with data showing that polymers with higher molecular weight reveal lower ablation rates.[37,38]

Conclusion

The ablation characteristics of various polymers were studied at low and high fluences. The polymers can be divided into three groups: polymers containing triazene groups and a cinnamylidenemalonyl group, the same polymers without the triazene group, and polyimide as reference polymer. At high fluences a very similar behavior, i.e., etch rates and effective absorption coefficients, was obtained for all polymers. The main difference is the absence of carbon deposits for all designed polymers. At low fluences very pronounced differences are detected. The polymers containing the photochemical most active group (triazene) are also the polymers with the lowest threshold of ablation and the highest etch rates, followed by the designed polyesters and then polyimide. No pronounced influences of the absorption coefficients, either α_{lin} or α_{eff}, on the ablation characteristics are detected. The thermal properties of the designed polymers are only of minor importance. The amount of detected gaseous products follows the same trend as the ablation activity, suggesting a combined mechanism of photochemical decomposition and associated volume increase (volume explosion) of the designed polymers. The clear difference between PI and the designed polymers might be explained by a pronounced thermal part in the ablation mechanism of PI.

Acknowledgment. We would like to thank Friederike Geiger for the EDX measurements. This work was financially supported by the Swiss National Science Foundation, Deutsche Forschungsgemeinschaft, and Deutscher Akademischer Austauschdienst.

References and Notes

(1) Srinivasan, R.; Mayne-Banton, V. *Appl. Phys. Lett.* **1982**, *41*, 576.
(2) Kawamura, Y.; Toyoda, K.; Namba, S. *Appl. Phys. Lett.* **1982**, *40*, 374.
(3) Suzuki, K.; Matsuda, M.; Ogino, T.; Hayashi, N.; Terabayashi, T.; Amemiya, K. *Proc. SPIE* **1997**, *2992*, 98.
(4) Lippert, T.; Stebani, J.; Ihlemann, J.; Nuyken, O.; Wokaun, A. *Angew. Makromol. Chem.* **1993**, *206*, 97.
(5) Lippert, T.; Stebani, J.; Ihlemann, J.; Nuyken, O.; Wokaun, A. *J. Phys. Chem.* **1993**, *97*, 12296.
(6) Lippert, T.; Kunz, T.; Hahn, C.; Wokaun, A. *Recent Res. Dev. Macromol. Res.* **1997**, *2*, 121.
(7) Nuyken, O.; Dahn, U., Hoogen, N.; Marquis, D.; Nobis, M. N.; Scherer, C.; Stebani, J.; Wokaun, A.; Hahn, C.; Kunz, Th.; Lippert, T. *Polym. News* **1999**, *24*, 257.
(8) Bennett, L. S.; Lippert, T.; Furutani, H.; Fukumura, H.; Masuhara, H. *Appl. Phys. A* **1996**, *63*, 327.
(9) Lippert, T.; Langford, S. C.; Wokaun, A.; Georgiou, S.; Dickinson, J. T. *J. Appl. Phys.* **1999**, *86*, 7116.
(10) Lippert, T.; Nakamura, T.; Niino, H.; Yabe, A. *Macromolecules* **1996**, *29*, 6301.

(11) Lippert, T.; Wei, J.; Wokaun, A.; Hoogen, N.; Nuyken, O. *Appl. Surf. Sci*. **2000**, *168*, 270.
(12) Kunz, Th.; Stebani, J.; Ihlemann, J.; Wokaun, A. *Appl. Phys. A* **1998,** *67*, 347.
(13) Wei, J.; Hoogen, N.; Lippert, T.; Hahn, Ch.; Nuyken, O.; Wokaun, A. *Appl. Phys. A* **1999**, *69*, S849.
(14) Lippert, T.; Wei, J.; Wokaun, A.; Hoogen, N.; Nuyken, O. *Macromol. Mater. Eng.* **2000,** *283*, 140.
(15) Seki, S.; Kanzaki, K.; Yoshida, Y.; Tagawa, S.; Shibata, H.; Asai, K.; Ishigure, K. *Jpn. J. Appl. Phys*. **1997**, *36*, 5361.
(16) Sadafule, D. S.; Panda: S. P. *J. Appl. Polym. Sci*. **1979**, *24*, 511.
(17) Hoogen, N.; Nuyken, O.; *J. Polym. Sci. Polym. Chem.* **2000**, *38*, 1903.
(18) Andrews, J. E. ; Dyer, P. E.; Forster, D.; Key, P. H. *Appl. Phys. Lett.* **1983**, *43*, 717.
(19) Srinivasan, R.; Braren, B. *J. Polym. Sci*. **1984,** *22*, 2601**.**
(20) Srinivasan, R. *Appl. Phys. A* **1993**, *56*, 417.
(21) Lazare, S.; Granier, V. *Chem. Phys. Lett*. **1990,** *168*, 593.
(22) Lazare, S.; Granier, V. *Appl. Phys. Lett*. **1989**, *54*, 862.
(23) Lippert, T.; Bennett, L. S.; Nakamura, T.; Niino, H.; Ouchi, A.; Yabe, A. *Appl. Phys. A* **1996**, *63*, 257.
(24) Pettit, G. H.; Sauerbrey, R. *Appl. Phys. A* **1993,** *56***,** 51.
(25) Furutani, H.; Fukumura, H.; Masuhara, H.; Lippert, T.; Yabe, A. *J. Phys. Chem A* **1997**, *101*, 5742.
(26) The etch rates were calculated to compare the polymers at identical fluences. The experimental data were taken at variable fluences, due to the variation of the laser energy between experiments.
(27) Defined as the fluence range where the onset of ablation could be measured with the profilometer.
(28) Tonyali, K.; Jensen, L. C.; Dickinson, J. T. *J. Vac. Sci. Technol. A* **1988**, *6*, 941.
(29) Dyer, P. E.; Jenkins, S. D.; Sidhu, J. *Appl. Phys. Lett.* **1986,** *49*, 453.
(30) Hopp, B.; Bor, Z.; Homolya, E.; Mihalik, E. *Proc. SPIE* **1998**, *3423*, 389.
(31) Raimondi, F.; Abolhassani, S.; Brütsch, R.; Geiger, F.; Lippert, T.; Wambach, J.; Wei, J.; Wokaun, A. *J. Appl. Phys.* **2000**, *88*, 1.
(32) Atkins, P. W. *Physical Chemistry*, 5th ed.; Oxford University Press: Oxford, UK, 1994.
(33) Lippert, T.; Stebani, J.; Stasko, A.; Nuyken, O.; Wokaun, A. *J. Photochem. Photobiol.* **1994**, *78*, 139.
(34) Ortelli, E. E.; Geiger, F.; Lippert, T.; Wei, J.; Wokaun, A. *Macromolecules* **2000**, *33*, 5090.
(35) Küper, S.; Brannon, J.; Brannon, K. *Appl. Phys. A* **1993**, *56*, 43.
(36) Arnold, N.; Bityurin, N. *Appl. Phys. A* **1999**, *68***,** 615.
(37) Lippert, T.; Wokaun, A.; Stebani, J.; Nuyken, O.; Ihlemann, J. *Angew. Makromol Chem.* **1993**, *213*, 127.
(38) Van Saarloos, P. P.; Constable, J. J. *J. Appl. Phys.* **1990**, *68*, 377.